

Pinch-Off Transition in Marangoni-Driven Thin Films

Andreas Münch

Institut für Mathematik, HU Berlin, D-10099 Berlin, Germany

(Received 14 April 2002; revised manuscript received 31 October 2002; published 3 July 2003)

We present a mathematical model and analysis for the pinch-off transition as observed in dip-coating experiments at the base of thin liquid films driven up a vertical plate by a thermally induced surface tension gradient with a counteracting gravitational force. Our results show that this transition gives rise to a complex new wave structure involving a nonclassical, *reverse* undercompressive shock wave.

DOI: 10.1103/PhysRevLett.91.016105

PACS numbers: 68.15.+e, 47.15.Gf, 47.20.Ky, 47.20.Ma

In this Letter, we revisit a fluid mechanical setting that has been very successful in supplying clear theoretical and experimental evidence for nonclassical, so-called “undercompressive shock waves” [1,2], which also play an important role in physical models from other fields that involve a scalar but high order convection/diffusion equation or certain kinds of systems of convection/diffusion equations. Here, we identify a new wave we call *reverse* undercompressive shock. It forms the trailing edge of a double shock wave in a thin liquid film that is driven up a plane by a thermally induced Marangoni shear stress, with a counteracting gravitational force. The double wave moves up the wafer similar to a solitary wave, thereby enclosing a certain amount of fluid. The velocity of the wave and the thickness of the enclosed film can be varied by changing the temperature gradient or the inclination angle, and the total amount of fluid by modifying the initial conditions.

These fluid dynamical properties make this novel structure an interesting mechanism for portioning and transporting miniature amounts of liquid in a microfluidic device. It shares an important feature with an earlier pumping design [3] which also makes use of the thermal dependence of surface tension and had a strong impact in the field [4], in that it requires no moving parts and no electrical fields. In addition, our mechanism works with much smaller temperature gradients. The work presented here provides the fundamental theory for the new double shock structure that is necessary to accurately predict and control the behavior in an actual application.

Undercompressive shocks violate the Lax condition [5] in that in the scalar case, characteristics pass through the shock path, rather than impinging on the shock trajectory from both sides (cf. [1], and references therein). In the past, these shock waves were often considered unphysical or at least highly unstable and were therefore excluded from the physically admissible solutions [5–7]. There is, however, a growing body of theoretical work indicating that undercompressive shocks do appear after all in solutions for various physical models. They occur in a modified Korteweg–de Vries–Burgers model for concentration

waves in suspensions of particles in fluids [8]. They also have been identified in a model for three phase flow (essentially an extension of the Buckley-Leverett equation) for water alternating gas recovery, for example, where they have a great practical potential for improving the efficiency of the recovery process [9].

Despite the theoretical evidence and potential practical implications, experiments targeted at identifying these undercompressive waves are comparatively scarce; where experimental data are available, they are often inconclusive (as in [8]) or still subject to debate. One of the important features of the Marangoni/gravity driven film is that, in contrast, a series of experiments [2,10] has clearly established the undercompressive shock as a fundamental feature of the flow.

Our theoretical results have already prompted new experimental work that confirms our predictions [11]. We hope this will further stimulate the interest in undercompressive shocks from researchers in other fields where these have been predicted.

The model.—We identified the new wave upon revisiting an old dip-coating experiment [12], where the substrate is vertically dipped into the reservoir of squalane and pulled out to the extent that the lower end of the substrate is connected to the bath by a liquid meniscus. The substrate is then subjected to a uniform thermal gradient, such that the temperature decreases towards its upper end. After a certain time interval, the thin film that moves out of the reservoir starts to pinch off just above the meniscus, giving rise to the new wave. The pinched-off portion of the film rises at about the rate of the leading wave, leaving a broadening region of essentially zero thickness behind it.

In order to investigate the wave formation from the beginning of the pinch-off, we need to include the meniscus region in our model. In [13], an extended lubrication model has been derived from the full Stokes/temperature equations by retaining the leading order terms (in terms of the capillary number) in the lubrication scalings *and* the leading order term in the scalings appropriate for the meniscus region. The resulting model for the film profile $z = h(x, t)$ (where x measures the

spatial coordinate along the plane in the upward direction and t represents the time),

$$h_t + [f(h)]_x = - \left[h^3 \left(\frac{h_{xx}}{[1 + (3\delta)^{4/3} h_x^2]^{3/2}} \right) \right]_x, \quad (1)$$

retains the full nonlinear curvature term $\kappa = h_{xx}/[1 + (3\delta)^{4/3} h_x^2]^{3/2}$ in the term on the right-hand side, which comes from surface tension. The quadratic and cubic terms in the flux function, $f(h) = h^2 - h^3$, are the contribution from the Marangoni stress and gravity, respectively. The small parameter $\delta = \tau/[2(\rho g \sigma)^{1/2}]$ is proportional to the square root of the capillary number $Ca = \mu U/\sigma$ based on the Marangoni velocity scale $U = \tau H/\mu$, where the variables h , x , and t have been nondimensionalized with $H = 3\tau/(2\rho g)$, $L = [3\sigma\tau/(2\rho^2 g^2)]^{1/3}$, and $\Theta = 2\mu(12\sigma\tau\rho g)^{1/3}/(3\tau^2)$, respectively. Here, ρ , σ , and μ are the liquid density, surface tension, and dynamic viscosity at a mean temperature \bar{T} , respectively, g is the gravitational acceleration, and τ is the surface tension gradient, i.e., $\tau = (d\sigma/dT)|_{\bar{T}} dT/dx$, where dT/dx is the (constant) temperature gradient imposed along the substrate.

The δ term can be neglected where the nondimensional slope h_x is small or moderate, i.e., in the thin film region, and (1) reduces to the lubrication model [14,2]

$$h_t + [f(h)]_x = -(h^3 h_{xxx})_x, \quad (2)$$

for which systematic investigations have shown that the interplay of the nonconvex flux function f and the high order smoothing term leads to double wave structures where the leading wave is a nonclassical, undercompressive shock [1]. Only in the meniscus region, where h_x becomes large, the δ term in (1) yields an $O(1)$ contribution.

For boundary conditions, we assume that the origin of our system of coordinates is chosen so that $x = 0$ is the level of the liquid surface far away from the plate. As x approaches the origin, the film profile passes over onto the surface of the liquid reservoir, i.e., $\lim_{x \rightarrow 0} h = \infty$. In the downstream direction, i.e., up the plate, $\lim_{x \rightarrow \infty} h = b$, for $b \neq 0$, in order to avoid the stress singularity at the moving contact line [15].

Numerical results.—The model equations are discretized on a finite domain using a standard finite difference scheme in space and an implicit method in time. For the purpose of presenting the numerical simulations and the sake of definiteness, we use as an example the physical parameters corresponding to trial four in the paper by Ludviksson and Lightfoot (LL) [12]: $\mu = 0.266 \text{ g s}^{-1} \text{ cm}^{-1}$, $\sigma = 27.8 \text{ g s}^{-2}$, $\tau = 0.128 \text{ g s}^{-2} \text{ cm}^{-1}$, $\rho = 0.805 \text{ g cm}^{-3}$, which yield $\delta = 0.431 \times 10^{-3}$, and $H = 2.43 \text{ } \mu\text{m}$, $L = 0.205 \text{ mm}$, and $\Theta = 350 \text{ s}$ for the two length scales and for the time scale. According to [1,2] for each height of the undercompressive front, here $h_{uc} = 0.733$, one can infer a unique value for b ; here $b = 0.0193$.

For the initial profile, we set

$$h(x, 0) = \begin{cases} b & \text{for } x_0 + x_i < x, \\ h_i & \text{for } x_0 < x \leq x_0 + x_i, \\ \frac{h_s[(3\delta)^{1/3}x]}{3\delta} + h_i & \text{for } 0 < x \leq x_0, \end{cases} \quad (3)$$

$$h_s(\xi) = \sqrt{2} - \sqrt{4 - \xi^2} + \ln \frac{(\sqrt{2} - 1)\xi}{2 - \sqrt{4 - \xi^2}},$$

where in dimensionless form $x_i = 101$ is the extension of the coating from the precursor to the tip of the meniscus located at $x_0 = \sqrt{2}/(3\delta)^{1/3}$, and $h_i = 12.4$ is the film thickness inferred from the removal rates via the Landau-Levich theory [16].

The numerical simulations of our model show two major phases in the evolution of the film. In the first phase, most of the wave of the initial film moves backwards and expands into a rarefaction wave, the thickest portions of which quickly reach the meniscus region and disappear into the dip/ridge that forms there at a very early stage. As thinner parts of the rarefaction wave arrive at the meniscus and disappear, the film thins as a whole. At the same time the leading front of the film profile begins to rise up the plate and the portion immediately behind it flattens out. In Fig. 1, one sees that there is a sizable flat stretch of constant thickness $h = h_{uc}$, between the right edge of the rarefaction wave (R) and the leading shock wave (UC). This is a sign that the rarefaction wave is separating off the leading shock wave, thereby indicating that the characteristic speed of the left state $f'(h_{uc})$ is lower than the shock speed. Indeed, as was discussed in detail in [17], UC is an undercompressive shock wave, with characteristics passing through the shock path from right to left.

At about $t = 115$ the evolution enters a second phase. The dip in the front part of the meniscus has thinned down until it reaches a minimum thickness, where it stops to decrease. The dip then widens and we see the formation of a trailing shock wave labeled RUC in the inset of Fig. 1.

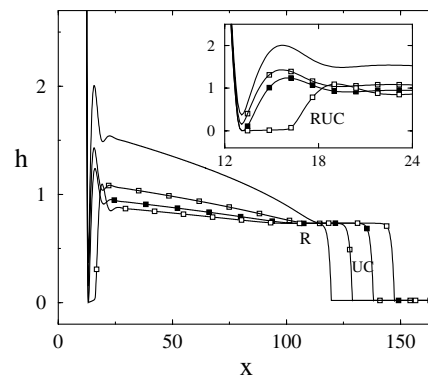


FIG. 1. Result of the simulation of LL's experiment, at dimensionless times $t = 23.0, 69.1, 115, 161$, corresponding to the solid line without symbols, the solid line with transparent, black, and opaque squares, respectively. The inset shows a close-up of the region near the origin, where the film pinches.

Both the leading and the trailing shock wave (UC and RUC) continue to rise up the substrate, leaving behind them a widening gap where the film is very thin, while the rarefaction wave (RW) gradually disappears into RUC.

It is argued in [14] that the pinch-off seen by LL is the process by which the meniscus establishes its equilibrium film thickness h_{eq} . This film thickness has also been observed for films rising onto a dry substrate, where the meniscus rapidly achieves a stationary state once the wave structures near the rising contact line have separated off the meniscus region. Once this has happened, the film portion between the waves and the meniscus is flat and of constant thickness h_{eq} , [18]. Approximations for h_{eq} can be derived through asymptotic considerations [14,13,19]. The matched asymptotic solution in [13] for the stationary extended lubrication model shows that logarithmic switchback terms appear in the next order correction for h_{eq} . We find that only for very small values of δ , such as used in this experiment, the value provided by the leading order asymptotic formula $h_{eq} = 6.41\delta = 2.76 \times 10^{-3}$ is sufficiently accurate.

As can be seen in Fig. 2 (dot-dashed lines), the minimum thickness that is achieved is indeed equal to h_{eq} . However, the figure also shows that the film in the “gap” is *not* uniformly flat, even after a long time has elapsed (Fig. 2, solid line, for $t = 1.09 \times 10^3$). Instead, we see the formation of a lower rarefaction wave (LRW), which connects a flat film portion in front of the meniscus to the left state of the second shock wave (RUC). Moreover, the leading edge of the rarefaction wave separates off the shock, thus indicating that the characteristics for the left state h_l are leaving the shock trajectory. Hence, the trailing shock wave is undercompressive, like the leading wave (UC), in that characteristics cross the shock path, but for the new wave RUC, the characteristics enter from the higher state and leave the shock trajectory for the lower state, $h_{uc} > h_l$. Therefore, we call it a reverse

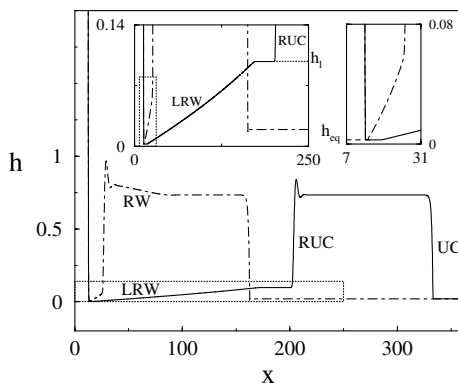


FIG. 2. Result of the simulation of LL’s experiment, at dimensionless times 238, 1.09×10^3 , corresponding to the dash-dotted and the solid line, respectively. The left inset shows an enlarged view of the region delimited by a box with dotted lines in the large figure. The right inset shows a close-up of the dotted box in the left inset.

undercompressive shock wave, RUC. This new undercompressive wave has a capillary ridge on top and a monotone profile towards the bottom. Conversely, the leading undercompressive wave is monotone at its top and has a dip where it connects to the precursor; see Fig. 4 for an enlarged view.

The wave pattern we observe in the simulation is largely determined by the possible shock waves, i.e., traveling wave solutions $h(x, t) = h_{tw}(x - st)$, for Eq. (1) or (2). Through application of phase space analysis to the resulting ordinary differential equation (ODE) for h_{tw} , we find that for a fixed right state h_{uc} (here = 0.733), Lax waves exist for a continuum of left states but only above a certain threshold, and an undercompressive wave for an isolated value h_l (here $h_l = 0.0980 > h_{eq}$) below the threshold, analogous to the situation for waves that connect to the precursor height b [1,21]. However, for any trailing Lax wave, the adjacent trailing rarefaction wave would move with characteristic speed and therefore merge with the Lax wave. Therefore this combination is not robust. This is in contrast to the combination with a reverse undercompressive wave, where the two waves separate, as seen in the simulations.

In addition to LL’s experiments, also those by [11] show that the film dynamics follows essentially the pattern described here for a wide range of parameters provided h_{eq} remains smaller than h_l , even for nonvertical plane positions. The newer experiments also confirmed our findings regarding the lower rarefaction wave, as well as the shape of the reverse undercompressive wave.

According to the Rankine-Hugoniot condition [1], a shock with left/right states h_{\pm} moves with speed $s = [f(h_-) - f(h_+)]/(h_- - h_+)$. The two parts of the double shock have h_{uc} as a common state but differ regarding their other states b and h_l , with $b < h_l < (1 - h_{uc})/2$, which implies that the reverse undercompressive wave travels faster. Therefore, in the setting of (1) with only one independent spatial coordinate, it will eventually catch up with the leading shock, and the double wave structure will disappear after a very long time. However, the difference between the two shock speeds is as small as 0.0118, so the merger will occur at about $t = 12 \times 10^3$, or 49 d. For the few hours during which LL’s observed two waves, the difference in the climbing rates is hardly

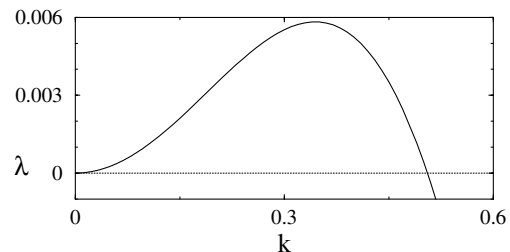


FIG. 3. Growth rate vs wave number for the reverse undercompressive wave connecting h_l and h_{uc} .

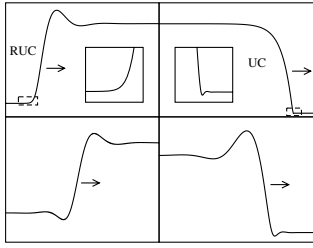


FIG. 4. Top row corresponds to parts of the solid line in Fig. 2, bottom row shows compressive waves of Figs. 8 and 4 in [1], respectively. Only the top right wave is stable [20].

noticeable, so that the pinched-off film would have appeared to move as a whole.

Stability of the reverse undercompressive wave.—We already know that the leading UC wave is stable with respect to spanwise perturbations [2]. Here, we investigate linear stability of the RUC wave; i.e., we consider it as a traveling wave solution of the two-dimensional version of (2),

$$h_t + [f(h)]_x = -\nabla \cdot (h^3 \nabla^3 h). \quad (4)$$

Like (2), this model is valid in the thin film away from the meniscus. The RUC wave is a one-dimensional solution of this equation of form $h(x, t) = H(X)$, $X = x - st$, with left and right states h_l and h_{uc} , respectively, where s is the wave speed. We note that by integrating once in X , one finds that H satisfies a third order ODE. We perturb $H(X)$ by $\epsilon g(X)e^{\lambda t + iky}$, $\epsilon \ll 1$, and linearize (3). The linearized equation is discretized and the resulting eigenvalue problem solved for the leading eigenvalue by inverse vector iteration. Figure 3 shows the result for the RUC wave in Fig. 2. One sees that for a range of wave numbers k , growth rates are positive, so that the RUC wave is unstable, in accordance with the observed “tears” behind the trailing wave [22] and also with the recent findings in [11].

Discussion.—In this Letter we argued that the pinch-off transition gives rise to a new wave structure involving a reverse undercompressive wave. To the best of our knowledge this is the first time this type of wave has been identified in an experimental situation for driven thin films. The stability properties of this new wave raises again the question of the underlying cause of linear instability in thin films. It has been argued in [18,23] that the pronounced capillary ridge is directly responsible for the appearance of the fingering instability. Figure 4 seems to underscore this suggestion, since it shows that all the traveling waves known to us up to now which are unstable do in fact have a pronounced capillary ridge. Conversely, the only wave that is stable is monotone except for a small dip.

Currently we are investigating the effect of nonvertical positions for the plate. As can be seen from earlier papers [13,24], this increases h_{eq} . We conjecture that for certain

ranges of inclination angles and choices of δ , the value of h_{eq} can be increased so that $h_{eq} > h_l$. In this case the rarefaction wave (LRW) cannot persist, since $f'(h) > f'(h_l)$ for a range of $h > h_l$.

Some preliminary results on the early stages of the pinch-off transition were published in [25], which was supported by the DFG stipend, MU 1626/1-1. A. M. was supported by the DFG research center “Mathematics for Key Technologies” (FZT 86) in Berlin.

-
- [1] A. L. Bertozzi, A. Münch, and M. Shearer, *Physica (Amsterdam)* **134D**, 431 (1999).
 - [2] A. L. Bertozzi, A. Münch, X. Fanton, and A. M. Cazabat, *Phys. Rev. Lett.* **81**, 5169 (1998).
 - [3] M. A. Burns *et al.*, *Proc. Natl. Acad. Sci. U.S.A.* **93**, 5556 (1996).
 - [4] D. D. Cunningham, *Anal. Chim. Acta* **429**, 1 (2001).
 - [5] P. D. Lax, in *CBMS-NSF Regional Conference Series in Applied Mathematics* (SIAM, Philadelphia, PA, 1973), Vol. 11.
 - [6] P. Germain, *Adv. Appl. Mech.* **12**, 131 (1972).
 - [7] R. Menikoff and B. J. Plohr, *Rev. Mod. Phys.* **61**, 75 (1989).
 - [8] A. Kluwick, E. A. Cox, and S. Scheichl, *Acta Mech.* **144**, 197 (2000).
 - [9] D. Marchesin and B. J. Plohr, *SPE J.* **6**, 209 (2001).
 - [10] M. Schneemilch and A. M. Cazabat, *Langmuir* **16**, 8796 (2001); **16**, 9850 (2001).
 - [11] J. Sur, A. L. Bertozzi, and R. P. Behringer, *Phys. Rev. Lett.* **90**, 126105 (2003).
 - [12] V. Ludviksson and E. N. Lightfoot, *Am. Inst. Chem. Eng. J.* **17**, 1166 (1971).
 - [13] A. Münch, *SIAM J. Appl. Math.* **62**, 2045 (2002).
 - [14] P. Carles and A.-M. Cazabat, *J. Colloid Interface Sci.* **157**, 196 (1993).
 - [15] E. B. Dussan and S. H. Davis, *J. Fluid Mech.* **65**, 71 (1974).
 - [16] L. Landau and B. Levich, *Acta Physicochim. URSS* **17**, 42 (1942).
 - [17] A. Münch and A. L. Bertozzi, *Phys. Fluids* **11**, 2812 (1999).
 - [18] A. M. Cazabat, F. Heslot, S. M. Troian, and P. Carles, *Nature (London)* **346**, 824 (1990).
 - [19] L. W. Schwartz, *J. Eng. Math.* **39**, 171 (2001).
 - [20] A. L. Bertozzi, A. Münch, M. Shearer, and K. Zumbrun, *Eur. J. Appl. Math.* **12**, 253 (2001).
 - [21] The traveling wave ODE has in fact been used to mathematically prove the existence of undercompressive waves for (2) in A. L. Bertozzi and M. Shearer, *SIAM J. Math. Anal.* **32**, 194 (2000); the proof also works for the reverse undercompressive wave.
 - [22] V. Ludviksson, Ph.D. thesis, University of Wisconsin, 1968.
 - [23] D. E. Kataoka and S. M. Troian, *J. Colloid Interface Sci.* **203**, 335 (1998).
 - [24] X. Fanton, A. M. Cazabat, and D. Quéré, *Langmuir* **12**, 5875 (1996).
 - [25] A. Münch, Habilitation thesis, TU Munich, 2001.